

FLOW PERIODICITY ANALYSIS OF LOW REYNOLDS NUMBER FLAPPING AIRFOILS

R. I. Zaman, J. C. S. Lai, J. Young and M. A. Ashraf

School of Engineering and Information Technology
 The University of New South Wales, Canberra ACT 2600, Australia

Abstract

Analysis of flow over low Reynolds number flapping airfoils is essential for maximizing the aerodynamic performance of Micro/Nano Air Vehicle (MAV/NAV) flight. Past research was mainly focused on finding the optimal kinematic parameters for maximizing thrust and propulsive efficiency. However, in the case of a pure plunging airfoil, it has been shown that by increasing the plunge velocity (kh , product of reduced frequency, k and plunge amplitude, h), the nature of force generation changes from periodic to chaotic [1-3]. For better stability and control of these vehicles, it is desirable to maintain periodic force generation. In the present study, the flow periodicity nature of a NACA0012 airfoil at Reynolds number $Re = 500$ undergoing pure pitch motion has been numerically simulated using the commercially available CFD package ANSYS FLUENT 14. In order to examine the flow periodicity, pure pitching motion has been simulated with instantaneous angle of attack profiles equivalent to those of pure plunge airfoils covering the transition from periodic to chaotic behaviour. The vortex dynamics and the effect of k on the transition of force generation (periodic to quasi-periodic) at larger pitching amplitudes are analysed. Results indicate that for a given k , increasing the pitching amplitude θ_0 increases mean thrust coefficient C_{Tmean} but as soon as the periodicity nature changes to quasi-periodic, C_{Tmean} drops because of the larger leading edge vortex (LEV) formation and their haphazard movement at high angle of attack (AoA).

Introduction

The concept of using flapping wings is drawn from Nature. Fish, cetaceans, birds and insects, dolphins and sharks have used flapping wings or fins for thrust and lift production for millions of years. Flapping wing aerodynamics has come into the spotlight after the evolution of requirements for Micro Air Vehicle (MAV) and Nano Air vehicles (NAV). Thrust generation by an oscillating airfoil undergoing pure plunge, pure pitch or combined pitch and plunge motion is very much dependent on the vortex dynamics in the wake of the airfoil. Optimum efficiency occurs when leading edge vortices (LEVs) and trailing edge vortices (TEVs) interact constructively [4]. Studies on pure plunge motion [5-7] shows that a plunging airfoil produces thrust above a critical kh of 0.1 [8].

Theodorsen [9] and Garrick [10] used linear theory to calculate theoretically the unsteady aerodynamic forces on a heaving and pitching airfoil in an ideal fluid. Garrick [10] showed that pure plunge motions generate thrust at all frequencies but pure pitch motions generate thrust only above some critical k at fixed θ_0 . For example, Koochesfahani's [11] experimental results confirmed Garrick's analysis that thrust production is possible at various θ_0 after a critical value of k been reached. For $\theta_0=4^\circ$, they showed that thrust is produced for $k>4$. Numerical studies [12, 13] confirmed that for θ_0 in the range $2\leq\theta_0\leq4$, increasing k produces higher thrust.

For greater agility, stability and control of MAVs, it would be desirable for the force generation to be periodic. Higher thrust can be achieved at high k and h values, however, higher kh would cause chaotic force generation by the airfoil.

Numerical studies by Lewin and Hariri [1] on pure plunge motion at $Re=500$ showed non periodic or asymmetric flow or a combination of both appears to occur when $kh\geq 0.8$. Ashraf et al. [3] showed that for pure plunge motion at $Re=20,000$, the nature of the force coefficients changes from periodic to non periodic for $kh>0.4$ and chaotic for $kh>1.25$.

The flow periodicity of pure pitch motion has not been previously explored. The objective of this study is, therefore, to examine the flow periodicity of a NACA0012 airfoil at $Re = 500$ undergoing pure pitch motion. The reduced frequency is taken at $k = \omega c/U_\infty = 4$ and 6, and $h = h_0/c = 0.040-0.25$ with the plunge velocity in the range of $0.24 \leq kh \leq 1.0$. Here, ω is the angular velocity, c is the chord length and U_∞ is the free stream velocity. The pitching axis is located at one-quarter of chord length from the leading edge. The Reynolds number of 500 is within the range of flight for insects and small birds and well within the laminar region. Equivalent instantaneous AoA (angle of attack) profiles are used in pure pitch simulations to enable comparisons with pure plunge motions. The vortex dynamics and the effect of pitching amplitude on the transition of force generation (periodic to chaotic) at larger kh values are analysed.

Computational Approach

Controlling Angle of Attack (AoA)

The sinusoidal motion of a plunging airfoil is expressed as:

$$Y(t) = h \sin(\omega t) \quad (1)$$

To maintain the instantaneous effective AoA for pure pitch motion $\theta(t)$ same as that for plunge motion ($\alpha(t)_{plunge}$):

$$\theta(t) = \alpha(t)_{plunge} = -\tan^{-1}\left(\frac{\dot{Y}}{U_\infty}\right) = -\tan^{-1}\left(\frac{\omega h \cos(\omega t)}{U_\infty}\right) \quad (2)$$

Solver

The unsteady incompressible laminar flow fields around a NACA0012 airfoil undergoing different kinematics are simulated using the commercially available CFD package 'ANSYS Fluent14.0'. Centre of Gravity (CG) motion was used to produce pitching or plunging motion of the airfoil through a User Defined Function (UDF) in the pre processor. The Navier-Stokes equations are solved with the two dimensional double precision pressure based solver, SIMPLE pressure-velocity coupling, least squares cell based gradients and second order upwind spatial discretization with a C-type grid.

Results and Discussions

Grid and Time Step Refinement

Prior to conducting detailed simulations, grid independence and time step independence tests were carried out at $Re=20,000$, $k=1.0$ and $h=0.25$ for pure plunge motion of a 2D NACA0012 airfoil. The velocity inlet boundary is 10 chords upstream from the leading edge (LE) of the airfoil and the pressure outlet boundary is 10 chords from the trailing edge (TE). The first grid point was located $0.0004c$. The grid refinement test was performed with grids 451×101 (201 points on the airfoil surface), 901×101 , 901×201 and 901×401 (401 points on the airfoil surface in each grid) with 800 time steps per cycle. The results for the thrust coefficient (C_T) averaged over the last 5 cycles out of 10 calculated cycles in table 1 shows that the 901×201 grid with 800 time steps is sufficiently refined.

For time independence tests, 400, 800 and 1600 time steps per cycle were used with the 901×201 mesh. Table 1 show that there is no variation in the increase of the number of time steps from 400 to 800 or 1600 time steps. Hence, 901×201 mesh with 800 time steps are used in all subsequent simulations.

Analysis	Grid Resolution	C_{Tmean}	Literature [3]	Error (%)
Grid Independence Test	451×101	0.023	0.025	8.0
	901×101	0.023	0.024	4.2
	901×201	0.024	0.025	4.0
	901×401	0.024	--	--
Time Independence Test	Time step no.			
	400	0.024	0.025	4.0
	800	0.024	0.025	4.0
	1600	0.024	0.025	4.0

Table 1. C_{Tmean} for different mesh resolutions and varying time steps.

Code Validation

In order to assess the quality of the mesh and methodology adopted here, calculations were made for a purely plunging airfoil. The variation of the computed C_{Tmean} with time agrees very well with that of Ashraf et al. [3], as shown in Figure 1.

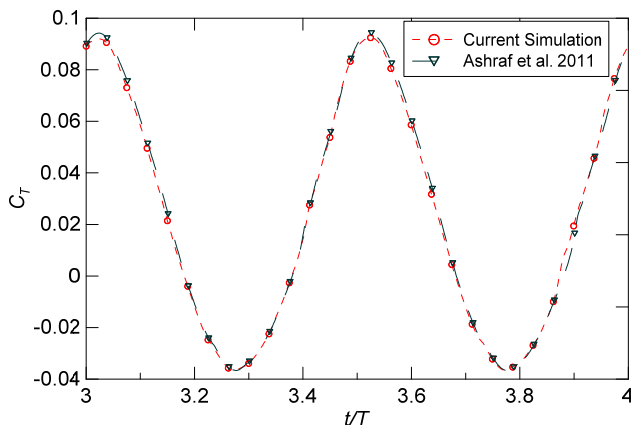


Figure 1. Comparison of computed instantaneous C_T with the results of Ashraf et al. [3]

Results Analysis

The equivalent instantaneous AoA for pitching motion has been calculated using equation (2). At $k=4$, $\theta_{max} = 13.5^\circ$, 21.8° and 30.9° , corresponding to plunge amplitudes $h=0.06$, 0.1 and 0.15 respectively. There have not been any studies of an airfoil

undergoing pure sinusoidal pitching motion for θ_o larger than 20° .

For pure pitch motion, Figures 2(a) and (b) show the variation of C_T with time, phase plots (C_T vs. lift coefficient, C_L) and power spectral density (PSD) of C_T for the last 15 cycles out of the 25 cycles calculated at $Re=500$, $k=4$, $\theta_{max} = 21.8^\circ$ and 30.9° corresponding to $h=0.1$ and 0.15 respectively.

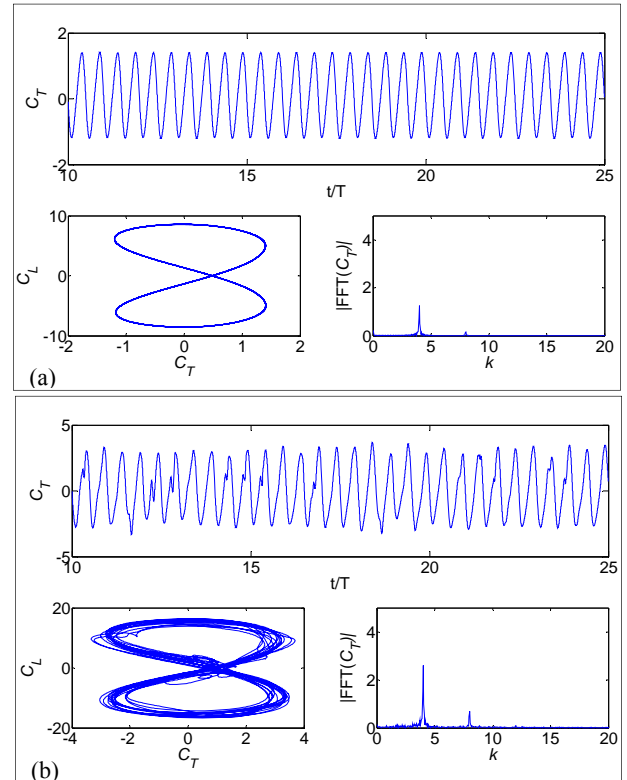


Figure 2: Time history of C_T , phase plot and power spectral density curve for different kinematics at $k=4$ and pitch amplitude (a) $\theta_{max}=21.8^\circ$ corresponding to $h=0.1$, $kh=0.4$, periodic and (b) $\theta_{max}=30.9^\circ$, corresponding to $h=0.15$, $kh=0.6$, quasi-periodic.

At $\theta_{max}=21.8^\circ$, the time history of C_T and the phase plot results in Figure 2(a) show that the behaviour of C_T is sinusoidal with only a single dominant peak in the PSD plot. As θ_{max} increases to 30.9° , Figure 2(b) shows a little deviation in the trajectory from cycle to cycle in the phase plot curve and a second frequency starts to appear in the PSD plot. Increasing θ_{max} to 58° , changes the force coefficient nature from quasi-periodic to chaotic and drag producing.

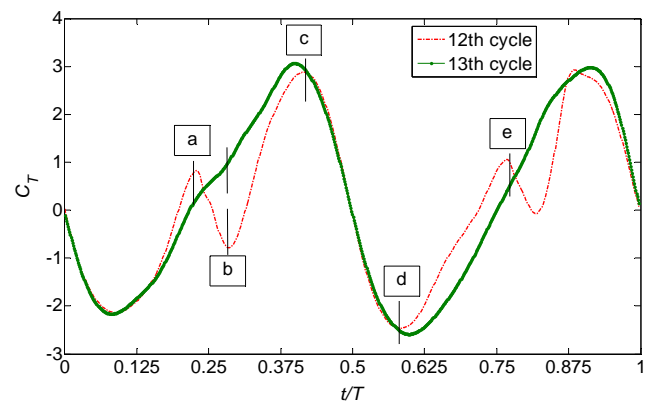


Figure 3: Time history of C_T for a NACA0012 airfoil in the 12th and 13th cycle undergoing pure pitch motion at $k=4$, $Re=500$ and $\theta_{max}=30.9^\circ$, $h=0.15$.

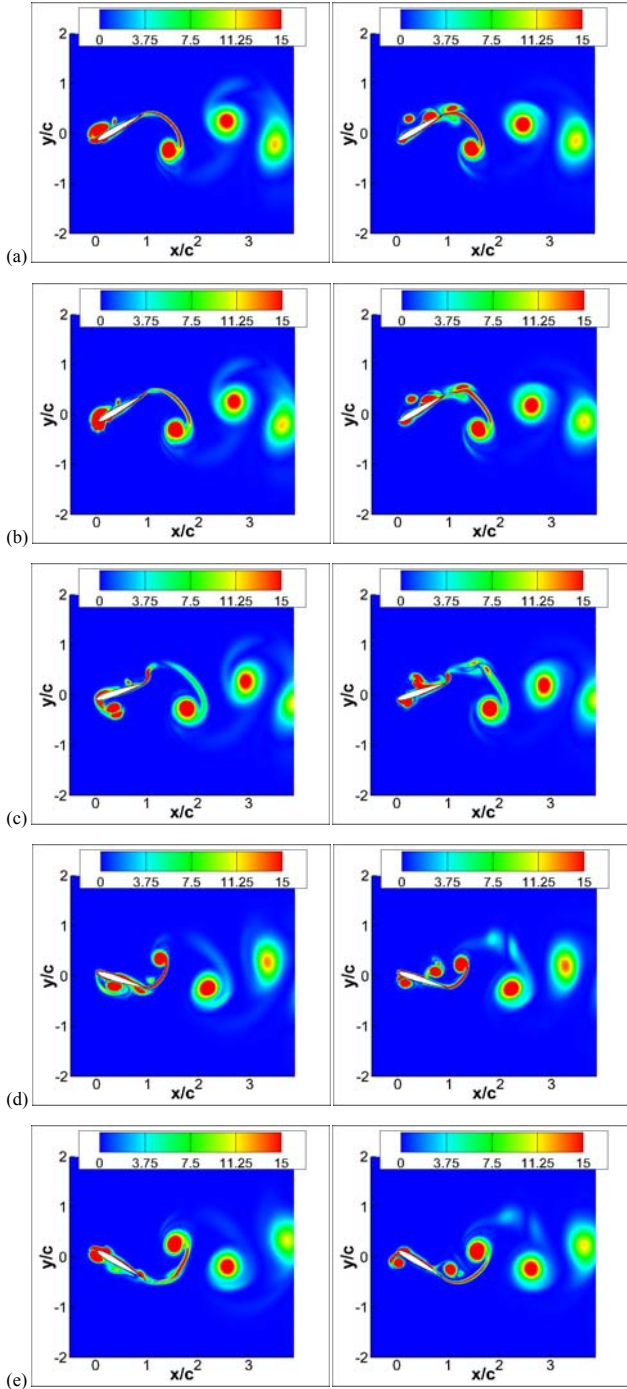


Figure 4: Comparison of instantaneous vortex field during 12th (left column) and 13th (right column) flapping cycle at $Re=500$, $k=4$, $\theta_{max}=30.9^\circ$ ($h=0.15$) (a) $t/T=0.22$, (b) $t/T=0.28$, (c) $t/T=0.4$, (d) $t/T=0.59$ and (e) $t/T=0.78$.

To identify the cause of quasi periodic force generation at, $k=4$, $\theta_{max}=30.9^\circ$, the variation of C_T with time for the 12th and 13th cycles is compared in Figure 3 while the vorticity field for the two cycles at different instants is compared in Figure 4. In both cycles, two larger TEVs form, strengthen and shed away in the wake. The major difference lies in the formation, movement and shedding of LEVs. In cycle 12, at $t/T=0.22$, i.e. point (a) on Figure 3, Figure 4(a) shows that a LEV forms and remains attached to the airfoil upstream of the point of maximum airfoil's maximum thickness and thus produce thrust [14]. But as the airfoil pitches further down, the airfoil surface hinders the free stream to flow over the surface of the airfoil as it lies almost normal to the suction force and causes drag force to occur as

shown in Figure 3. At $t/T=0.28$, i.e. point (b) on Figure 3, the local minimum drag occurs in the 12th cycle after which the drag starts decreasing towards thrust. Figure 4(b) shows that the attached LEV actually starts to slide down from the upper surface to the lower surface of the airfoil. Since the LEV portion in the lower surface does not block the free stream suction from the upstream side of the airfoil, C_T starts to increase from this point onwards up to point (c) i.e. $t/T=0.4$; after which the LEV is no longer connected to the LE and shed from the lower surface which causes the drop in C_T value. The drop in C_T continues to increase until the pitch up starts and an LEV starts to develop in the LE at $t/T=0.59$ and C_T starts to increase again but due to a LEV attached to the aft maximum thickness in the bottom surface of the airfoil, thrust cannot increase sharply because of the presence of drag. At point (e), i.e. $t/T=0.78$, the LEV accumulated and attached at the LE but because of pitching up motion, the bottom surface lies almost normal to the suction force due to LEV which hinders the thrust to generate similar to point (b).

In 13th cycle, at $t/T=0.22$, there are LEVs break into parts and shed away from the airfoil which convect downstream to the TE. But they are very small in size and do not affect the reverse von Kerman vortex in the wake which shows thrust. At $t/T=0.28$ i.e. point (b), one of the previously shed LEV convects downstream reattaches to the trailing edge (TE) and this LEV sucks free stream fluid from the downstream side and reduces thrust slightly, representing a little dip at point (b) in figure 3. At $t/T=0.4$, the connected LEV at the LE is just waiting to be shed from the airfoil which causes drop in C_T from point (c) onwards. Also the attached airfoil in the aft maximum thickness of the airfoil causes drag to strengthen. At $t/T=0.59$ during pitch up motion, a LEV starts to form at the upper surface of the LE. This LEV remains attached to the airfoil and as a result increases the C_T from the point (d) and C_T value continues to increase as the LEV grows larger in point (e).

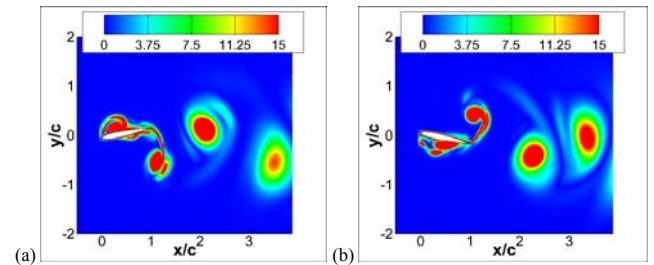


Figure 5: Instantaneous vorticity contour during (a) 12th cycle, $t/T=0.53$ (pitching down), and (b) 13th cycle, $t/T=0.03$ (pitching up) both at $k=4$, $\theta_{max}=45^\circ$ and $h=0.25$.

To study the force generation at higher θ_{max} of 45° two conditions has been examined in figure 5(a) and (b) for $k=4$ and $\theta_{max}=45^\circ$. At this kinematic, the pitching up and down motion causes the LEV to attach to the aft maximum thickness in each half cycle. This phenomenon causes the drag force production for a longer period of time during one half cycle and as a result, the net force coefficient value becomes negative. Figure 5(a) shows that during 12th cycle at $t/T=0.53$, the previously shed LEV attaches again to the upper mid surface of the airfoil and causes drag. As soon as the attached LEV slides to the upstream maximum thickness, thrust starts to produce from it. Similarly, Figure 5(b) shows the same phenomenon during pitch up motion in the 13th cycle.

From the above discussion it is apparent that the movement of the LEVs and their reattachment to the airfoil surface in the aft maximum thickness prolongs the drag production in one cycle and causes net drag at $\theta_{max}>30.9^\circ$.

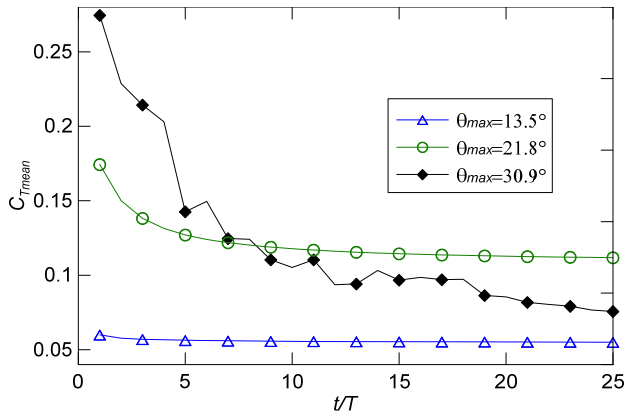


Figure 6: C_{Tmean} for pitching NACA0012 airfoil at $k=4$ and $\theta_{max} = 13.5^\circ$, 21.8° and 30.9° respectively.

Figure 6 shows the time varying C_{Tmean} for different θ_{max} at $k=4$ as each cycle progresses. The C_{Tmean} value starts to increase with increase in θ_{max} . Previous study by Lee et al. [12] shows that at $Re=5000$ with a $\theta_o=20^\circ$ and $k=8$, an airfoil undergoing pure pitching motion can generate $C_{Tmean} = 0.95$.

Kinematics ($k\theta_{max}$ in radian)		C_{Tmean}	Periodicity Nature
$k=4$	$\theta_{max} = 13.5^\circ$ ($k\theta_{max}=0.94$)	0.055	Periodic
	$\theta_{max} = 21.8^\circ$ ($k\theta_{max}=1.52$)	0.118	Periodic
	$\theta_{max} = 30.9^\circ$ ($k\theta_{max}=2.16$)	0.076	Quasi
	$\theta_{max} = 45.0^\circ$ ($k\theta_{max}=3.14$)	-1.118	Chaotic
	$\theta_{max} = 58.0^\circ$ ($k\theta_{max}=4.05$)	-7.076	Chaotic
$k=6$	$\theta_{max} = 13.5^\circ$ ($k\theta_{max}=1.41$)	0.272	Periodic
	$\theta_{max} = 21.8^\circ$ ($k\theta_{max}=2.28$)	0.653	Quasi
	$\theta_{max} = 45.0^\circ$ ($k\theta_{max}=4.72$)	-1.183	Chaotic
$k=8$	$\theta_{max} = 19.8^\circ$ ($k\theta_{max}=2.76$)	1.311	Quasi

Table 2: C_{Tmean} for the last 20 cycles out of 25 cycles calculated for a pitching NACA0012 airfoil at $Re=500$ and $k=4$.

Table 2 shows the periodicity nature and C_{Tmean} for different $k\theta_{max}$ ($0.94 \geq k\theta_{max} \geq 4.72$). At low θ_{max} ($k=4$ and $k\theta_{max}=0.94$), the time variation of C_T is periodic because of low AoA and small LEV formation. Increasing $k\theta_{max}$ up to 1.52 shows periodic flow behaviour and thrust producing. $k\theta_{max} \geq 2.16$ at $k=4$ causes larger LEV formation and quasi-periodic force generation and finally at $k=4$ and $k\theta_{max} \geq 3.14$, only net drag is produced with chaotic flow behaviour. From table 2, we can see that at $\theta_{max}=13.5^\circ$, increasing k from 4 to 6 increases the C_{Tmean} by 4.95 times which is in good agreement with previous studies [11-13] on pure pitching motion that increasing k for a particular θ_{max} increases C_{Tmean} because at higher k , LEVs has very little effect and TEVs are the dominant vortices which result in jetlike flow from the TEVs only [12]. But in case of high $\theta_{max} \geq 20^\circ$, the LEVs shall not disappear with increasing k .

Conclusions

A numerical analysis of the flow periodicity of flapping 2D NACA0012 airfoil at $Re = 500$ undergoing pure pitch motion has been studied for $k=4$ and 6. For a given k , it has been shown that increasing θ_{max} increases C_{Tmean} ($k=4$ and 6). The results also show that for a given θ_{max} , increasing k increases the C_{Tmean} but shifts the periodicity nature from periodic to quasi-periodic similar to pure plunge motion. We shall further explore our analysis to find the effect of increasing k at higher θ_{max} to look for the possibility of achieving thrust and for low θ_{max} , how much further can we push the k for generating thrust from it.

Acknowledgements

The first author (RIZ) acknowledges receipt of a University College Postgraduate Research Scholarship for the pursuit of this study.

References

- [1] Lewin, G. C., and Haj-Hariri, H. "Modelling Thrust Generation of a Two-dimensional Heaving Airfoil in a Viscous Flow," *Journal of Fluid Mechanics* Vol. 492, 2003, pp. 339-362.
- [2] Lentink, D., Muijres, F. T., Donker-Duyvis, F. J., and Leeuwen, J. L. v. "Vortex-Wake Interactions of a Flapping Foil that Models Animal Swimming and Flight," *The Journal of Experimental Biology* Vol. 211, 2008, pp. 267-273.
- [3] Ashraf, M. A., Young, J., and Lai, J. C. S. "Oscillation Frequency and Amplitude Effects on Plunging Airfoil Propulsion and Flow Periodicity," *AIAA Journal* (Accepted), 2011.
- [4] Anderson, J. M., Streitlien, K., Barrett, D. S., and Triantafyllou, M. S. "Oscillating Foils of High Propulsive Efficiency," *Journal of Fluid Mechanics*, 1998, pp. 41-72.
- [5] Lai, J. C. S., and Platzer, M. F. "Jet Characteristics of a Plunging Airfoil," *AIAA Journal* Vol. 37, No. 12, 1999, pp. 1529-1537.
- [6] Platzer, M. F., Jones, K. D., Young, J., and Lai, J. C. S. "Flapping Wing Aerodynamics: Progress and Challenges," *AIAA Journal* Vol. 46, No. 9, 2008, pp. 2136-2149.
- [7] Young, J., and Lai, J. C. S. "Oscillation Frequency and Amplitude Effects on the Wake of a Plunging Airfoil," *AIAA Journal* Vol. 42, No. 10, 2004, pp. 2042-2052.
- [8] Ashraf, M. A., Lai, J. C. S., and Young, J. "Numerical Analysis of Flapping Wing Aerodynamics," *16th Australasian Fluid Mechanics Conference*. Crown Plaza, Gold Coast, Australia, 2007, pp. 1283-1290.
- [9] Theodorsen, T. "General Theory of Aerodynamic Instability and the Mechanism of Flutter," *NACA Report* 1935.
- [10] Garrick, I. E. "Propulsion of a Flapping and Oscillating Airfoil," *NACA Report -567*. 1937.
- [11] Koochesfahani, M. M. "Vortical Patterns in the Wake of an Oscillating Airfoil," *AIAA Journal* Vol. 27, No. 9, 1989, pp. 1200-1205.
- [12] Lee, J.-S., Kim, C., and Kim, K. H. "Design of Flapping Airfoil for Optimal Aerodynamic Performance in Low-Reynolds Number Flows," *AIAA Journal* Vol. 44, No. 9, 2006, pp. 1960-1972.
- [13] Sarkar, S., and Venkatraman, K. "Numerical Simulation of Thrust Generating Flow Past a Pitching Airfoil," *Computers & Fluids* Vol. 35, No. 1, 2006, pp. 16-42.
- [14] Young, J., and Lai, J. C. S. "On the Aerodynamic Forces of a Plunging Airfoil," *Journal of Mechanical Science and Technology* Vol. 21, No. 9, 2007, pp. 1388-1397.